Asian Journal of Pharmaceutical Sciences 18 (2023) 100777

Available online at www.sciencedirect.com

ScienceDirect

journal homepage: www.elsevier.com/locate/AJPS

Original Research Paper

An intra-articular injectable phospholipids-based gel for the treatment of rheumatoid arthritis

Yuping Yang[a], *Shiqin Luo*[a], *Xiong Peng*[a], *Ting Zhao*[a], *Qin He*[a,b], *Mengying Wu*[a], *Wei Zhang*[a], *Tao Gong*[a,*], *Zhirong Zhang*[a]

[a] *Key Laboratory of Drug-Targeting and Drug Delivery System of the Education Ministry and Sichuan Province, Sichuan Engineering Laboratory for Plant-Sourced Drug and Sichuan Research Center for Drug Precision Industrial Technology, West China School of Pharmacy, Sichuan University, Chengdu, 610064, China*

[b] *Department of Pharmacy, West China Hospital Sichuan University Jintang Hospital, Chengdu, 610000, China*

ARTICLE INFO

Article history:
Received 30 July 2022
Revised 28 November 2022
Accepted 10 January 2023
Available online 18 January 2023

Keywords:
Celastrol
Rheumatoid arthritis
Phospholipids-based controlled release gel
Intra-articular drug delivery

ABSTRACT

Rheumatoid arthritis (RA) is a chronic inflammatory and destructive arthropathy with a high deformity rate. Despite numerous studies and clinical trials, no curative treatment is available for large weight-bearing joints. Intra-articular (IA) injections could deliver high concentrations of drug to the afflicted joint and improve the drug efficacy while reducing systemic toxicity. However, free drugs are rapidly cleared from synovial fluid and do not significantly halt the progression of joint disease. Herein, a phospholipids-based controlled-release gel was prepared for sustained IA delivery of celastrol (CEL) and the therapeutic efficiency was evaluated in a rheumatoid arthritis rabbit model. The CEL-loaded gel (CEL-gel) contained up to 70% phospholipids yet was easy to inject. After injecting into the joint cavity, CEL-gel achieved sol to gel phase transition without special stimuli and gelling agent. *In vitro* release and *in vivo* pharmacokinetic studies evidenced the stable and sustained release action of CEL-gel. A single IA injection of CEL-gel could maintain therapeutic efficiency for about 25 d and showed much better anti-arthritic efficacy compared to repeated injections of free drug solution (CEL-sol). Furthermore, the IA injection of CEL-gel greatly reduced the systemic toxicity of CEL. With good biocompatibility and biodegradability, CEL-gel might be a promising IA drug delivery system.

1. Introduction

Rheumatoid arthritis (RA) is the most common chronic autoimmunity-related disease that causes progressive joint inflammation related to synovial vascular hyperplasia, cartilage destruction and bone erosion. RA affected 0.5%–1% of the world's adults and the long-term prognosis was bleak, 80% of symptomatic patients were disabled after 20 years. When RA affects large weight-bearing joints, nearly

* Corresponding author.
E-mail address: gongtaoy@126.com (T. Gong).
Peer review under responsibility of Shenyang Pharmaceutical University.

https://doi.org/10.1016/j.ajps.2023.100777

all patients have movement limitations and even cannot perform daily activities [1]. In the microenvironment, local immune cells including macrophages, T-cells and monocytes overexpress numerous pro-inflammatory cytokines such as tumor necrosis factor-α (TNF-α), interleukin-1 (IL-1) and interleukin-6 (IL-6), leading to the flares of RA [2]. Those cytokines further irritate synovial fibroblasts, osteoclasts and chondrocytes to release matrix metalloproteinases-3 (MMP-3) and other effector molecules, causing erosion of bone and cartilage [3]. Therefore, a sensible therapeutic method that alleviates those symptoms is urgently required. The goals of large joints arthritis treatment are to halt disease progression, suppress synovial inflammation, prevent cartilage and bone damage, and restore joint mobility and function. Traditional RA therapy strategies include the administration of disease-modifying antirheumatic medicines (DMARDs), nonsteroidal anti-inflammatory medications (NSAIDs) and glucocorticoids (GCs). However, long-term use of those drugs merely provides limited benefits and usually comes with a series of unbearable side effects. In recent years, biological DMARDs such as anti-TNF treatment were efficient in the early stage of the disease. However, a relatively large population of patients also fails to respond to these treatments [4].

Celastrol (CEL) as a natural bioactive compound extracted from traditional Chinese medicine *Tripterygium wilfordii* shows excellent anti-rheumatic activity. Multiple pro-inflammatory cytokines, including TNF-α, IL-1β and IL-6 were proven to be down-regulated by CEL through inhibition of the nuclear factor kappa B (NF-κB) signal transmission pathway [5–8]. It has been identified in numerous studies that CEL reduces synovial inflammation and attenuates bone erosion in experimental arthritis models [9–13]. However, severe toxicity and unsatisfactory oral bioavailability limited the application of CEL in the clinic [14–17]. Thus, we hypothesized that direct delivery of CEL into the joint cavity might reduce systemic exposure and improve bioavailability.

IA injection reduces the dosage used compared with systemic administration. Yet despite IA injection, symptom improvement of RA is usually temporary because the free CEL quickly leaves the joint cavity and distributes all across the body [18,19]. Arthritis sufferers need regular administration and those severe patients require it on daily basis. The ongoing IA injections might greatly reduce patient compliance. Thus, reducing the times of injections to intervals of a month might be of great help to clinical IA treatment. Although numerous formulations have been reported, there just a few agents are licensed for IA treatment due to special limitations, such as rapid distribution, elicit inflammation, instability and so on [20–22].

The gel delivery system has been widely studied and applied for its excellent sustained release capabilities in the past decade years [23–25]. Phospholipids-based gel system, previously constructed in our laboratory, could achieve 30 d of sustained release subcutaneously (SC) [26]. We consequently assume that developing phospholipids-based gel for IA injection may realize local sustained delivery of CEL to improve large joint arthritis. The phospholipids-based gel system that we constructed was a transparent solution with low viscosity *in vitro*, after injecting into the joint cavity, the sol-gel transition happened because ethanol diffused out from the gel and the water from synovial fluid diffused into it. With poor water solubility, the precipitation of phospholipids blocked the rapid release of CEL. Along with the exchange of ethanol-synovial fluid and metabolic degradation of the gel skeleton, CEL was released to relieve local arthritic pain. Which also reduced the CEL total dose and minimized systemic side effects. In this study, morphology, viscosity, release profile, and storage stability were investigated *in vitro*. Pharmacokinetic and therapeutic efficacy was further investigated *in vivo*.

2. Materials and methods

2.1. Materials

Celastrol (CEL) was purchased from Chengdu Must Bio-Technology (Chengdu, China). Phospholipid (Soya Phosphatidyl Choline, S100) was provided by Lipoid (Ludwigshafen, Germany). Injection-level medium-chain triglyceride (MCT) was supplied by Yuanye Bio-Technology Co., Ltd. (Shanghai, China). Absolute ethyl alcohol (analytical-grade) was purchased from Shiyang Chemical Reagent Factory (Chengdu, China). Ovalbumin (OVA) and Complete Freund's adjuvant (CFA, 1 mg/ml) were purchased from Sigma-Aldrich, St., Louis (MO, USA). 4% paraformaldehyde was purchased from Bio-sharp (Hefei, China). NP-40 lysis buffer was purchased from Beyotime Bio-Technology Co., Ltd (Shanghai, China). Protease Inhibitor Cocktail was purchased from APExBIO (TX, USA). All enzyme-linked immunosorbent assay (ELISA) kit was purchased from Ruixin Biotechnology Co., Ltd (Quanzhou, China). Other reagents and solvents were analytical and HPLC grade.

2.2. Animals

Healthy male New Zealand rabbits (2.2–1.8 kg) from the Dashuo Biological Technology Co., Ltd (Jianyang, Chengdu, China) are raised in a temperature and humidity-controlled environment. All animal-related procedures were carried out by the requirements of the National guidelines and were approved by the Animal Care and Ethics Committee of Sichuan University.

2.3. Preparation and characterization of CEL-gel

The CEL-gel was prepared by utilizing a magnetic stirring method with S100, MCT and ethanol in a ratio of 70: 15: 15 (w/v/v) (or 75: 10: 15, 65: 20: 15 or 60: 25: 15). CEL was dissolved with 0.15 ml ethanol and 0.15 ml (or 0.1, 0.2 or 0.25 ml) MCT in a vial. Then 0.7 g (or 0.75 g, 0.65 g or 0.6 g) S100 was added and the compound was stirred at 25 °C for 1 h. The pre-CEL-gel (state before CEL-gel gelation) was obtained after filtering through a 0.22 μm microfiltration membrane.

To characterize the sol to gel transition of CEL-gel *in vitro*, dialysis bags were used to simulate the ethanol-body fluid exchange process. 10 ml pre-CEL-gel was added to a dialysis bag (MWCO 8 kD - 14 kD) and immersed in 100 ml pre-warmed phosphate-buffered saline (PBS, 0.01 M, pH = 7.4),

then the gelation from sol to gel finished after 30 min [27]. The viscosity of CEL-gel before and after the transition as well as the viscosity with different S100 contents were measured at room temperature by a rotational viscometer (Brookfield DV-Rotational Engineering Laboratories, Inc., USA).

To observe the microscopic morphology of CEL-gel *in vivo*, we injected pre-CEL-gel into the joint cavity of rats. After 30 min, the rats were sacrificed to take out the CEL-gel, and the samples were observed by scanning electron microscopy (SEM, Inspect, FEI, USA).

2.4. *In vitro release study*

The *in vitro* release behaviors of CEL-gel were evaluated by the dialysis method in release mediums including 3% DMSO, 30% ethanol, and 50% ethanol in PBS (containing 4% Tween 80, v/v) respectively [28]. The pre-CEL-gel (2 mg/ml) was prepared as described above. And the free CEL solution (CEL-sol, 2 mg/ml) as a control was obtained by dissolving 20 mg CEL in a mixture of 300 μl DMSO and 2 ml anhydrous ethanol, then slowly adding PBS (containing 4% Tween 80) to 10 ml under water bath sonication. After preparing, pre-CEL-gel (0.5 ml) or CEL-sol (0.5 ml) was added into the dialysis bag (MWCO 8 kD - 14 kD) and immersed in 5 ml of pre-warmed release medium at 37 °C with shaking at 100 rpm. At pre-determined time intervals (0.25 h, 0.5 h, 1 h, 2 h, 3 h, 4 h, 6 h, 8 h, 12 h, 24 h, 36 h, 48 h, 60 h, 3 d, 3.5 d, 4 d, 5 d, 6 d, 8 d, 10 d, 13 d, 16 d, 19 d, 22 d), all release media was taken out and replaced by 5 ml of fresh release medium [29]. The sample was diluted by methanol and the concentration of CEL was analyzed by HPLC (Agilent 1260 infinity, USA) with an ODS column (Kromasil C_{18}, 5 μm, 150 mm × 4.6 mm). The mobile phase consisted of 95% methanol and 5% 0.1 M sodium dihydrogen phosphate water solution. The sample was analyzed at 425 nm and the ODS column temperature was kept at 35 °C [15]. The cumulative release rate of CEL was calculated and drawn by Graphpad 5.0 software (USA).

2.5. *Pharmacokinetic study*

The pre-CEL-gel (2 mg/ml) and CEL-sol (2 mg/ml) were prepared as described above. Healthy ten male New Zealand rabbits (1.8 - 2.2 kg) were divided into two groups (n = 5): pre-CEL-gel and CEL-sol with IA injection at an equal dose of CEL at 1 mg/kg (0.5 ml each knee). After injection, blood was collected from rabbit ear vein by heparinized tubes at pre-determined time points (0.5 h, 1 h, 2 h, 4 h, 8 h, 12 h, 24 h, 48 h, 4 d, 6 d, 9 d, 12 d, 15 d, 20 d, 25 d). The samples were centrifuged immediately at 5000 rpm for 6 min to collect 200 μl plasma [30]. The concentration of CEL in plasma was monitored by liquid chromatography-mass spectrometry (LC-MS/MS, Agilent Technologies Co. Ltd., USA). Data processing and analysis were carried out in DAS 3.2.5 software (China) and Graphpad 6.0 software (USA) [31,32].

2.6. *Storage stability study of CEL-gel*

Briefly, the prepared pre-CEL-gel was divided into different sample bottles, then argon was injected into the upper part of the bottle to prevent oxidation. The bottles were put at 4 °C. At pre-determined time intervals (0 d, 1 d, 3 d, 5 d, 7 d, 10 d, 14 d, 18 d, 21 d, 28 d), three sample bottles were taken out and 50 mg pre-CEL-gel was withdrawn from bottles for content determination [33]. Similarly, 50 mg pre-CEL-gel was taken out from the upper and lower parts of the vials on Day 0 and 28 for drug-dispersion uniformity analysis. The concentration of CEL was monitored by HPLC as the above method and the concentration-time profiles were calculated and plotted. Viscosity data before (0 d) and after (28 d) storage was also measured at 25 °C.

2.7. *Establishment of antigen-induced arthritis (AIA) model in rabbit*

Chronic arthritis was induced in immunized rabbits by repeated injections of OVA and CFA. The detailed protocol of AIA induction and IA treatment with CEL in rabbits was shown in Table 1 and Fig. 5A. Briefly, OVA was dissolved in PBS (20 mg/ml) and mixed with an equivalent volume of CFA. Then the mixture was emulsified completely at 4 °C. Rabbits were weekly immunized by injecting 1 ml emulsion at five sites in the subcutaneous of the back for three weeks. In the fourth week, the mixed OVA/CFA emulsion was injected into the bilateral knee joints (0.5 ml per knee) to induce the AIA rabbit model [34–38]. The injection of sterile 0.9% saline was done as a control.

2.8. In vivo *therapeutic efficacy evaluation*

The anti-RA effect of CEL-gel was evaluated in the AIA rabbit model established above. Firstly, the pre-CEL-gel (8 mg/ml) was prepared as described above. And the CEL-sol (0.8 mg/ml) was obtained by dissolving CEL in PBS (containing 0.3% DMSO, 9% ethanol, and 0.5% Tween 80). Briefly, 18 AIA rabbits were stochastically divided into three groups (n = 6): CEL-gel, CEL-sol, and normal saline. The CEL-gel group was single intraarticularly injected with 0.5 ml pre-CEL-gel (at the dose of 3.2 mg/kg) in each knee joint. At the same time, the equivalent volume of CEL-sol (at the dose of 0.32 mg/kg) was administrated by IA injection every 2 d for 21 d Joint diameter and joint skin temperature were recorded during CEL administration.

2.8.1. *Detection of cytokines level after therapy*

After 21 d treatment, rabbits in all groups were sacrificed. The blood was harvested by tubes to obtain serum. Meanwhile, the synovial membrane of the knee was stripped, homogenized in lysis buffer with protease inhibitor cocktail, and centrifuged at 10,000 rpm for 30 min to yield supernatant. All samples were refrigerated at −40 °C before determination. The concentration of the transcription factor NF-κB and cytokines including TNF-α, IL-1β and IL-6, and MMP-3 in serum and knee tissue were measured using ELISA kits.

2.8.2. *Histological of knee joints at the end of therapy*

The knee joints obtained from rabbits then were fixed in 4% paraformaldehyde. Half knee joints from each group were decalcified in 10% neutral formaldehyde-EDTA decalcification

Table 1
Induction of antigen-induced arthritis (AIA) in rabbits.

Day	Procedure	OVA (mg/per rabbit)	CFA (ml/per rabbit)	Injection site
−28	Immunization	10	0.5	SC
−21	Immunization	10	0.5	SC
−14	Immunization	10	0.5	SC
−7	IA Injection	10	0.5	IA
0	CEL formulation treat	–	–	IA

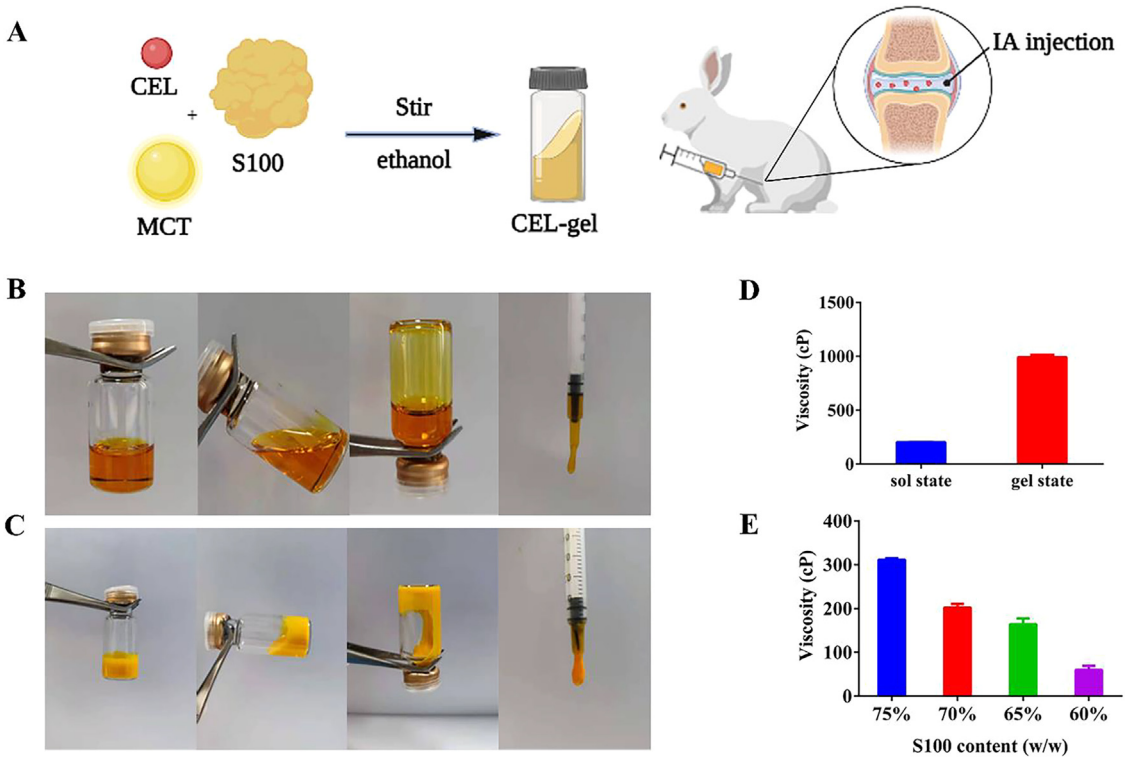

Fig. 1 – (A) Simple diagram of pre-CEL-gel formulation and delivery way. Morphology of CEL-gel before (B) and after (C) gelation. (D) The viscosity of CEL-gel in sol and gel states at 25 °C ($n = 3$). (E) The viscosity of pre-CEL-gel at 25 °C with different S100 concentrations ($n = 3$).

solution at 37 °C for 3 months. The decalcified joints were stained with Toluidine blue and hematoxylin-eosin (H&E) [39]. Staining was observed by a microscope (Olympus BX53, Tokyo, Japan).

2.8.3. *Micro-CT analysis and bone assessment*

The remaining half of knee joints collected at the end of therapy were scanned by an *ex vivo* micro-computed tomography (micro-CT, VivaCT80, SCANCO Medical AG, Switzerland). The scan parameters were 70 kV, 114 μA, and 8 W with a resolution of 35 μm. The 3D pictures of the knee joints were then reconstructed, and bone morphometric parameters including bone mineral density (BMD), trabecular number (Tb. N), and trabecular separation (Tb. Sp) were also quantitatively calculated.

2.9. *Safety evaluation*

To verify that CEL-gel can reduce the systematic toxicity of CEL, each leg of healthy male New Zealand rabbits (1.4–1.6 kg) was given IA injections of 0.5 ml saline, vehicle (blank-gel) or pre-CEL-gel (3.2 mg/kg). The free CEL group received 0.5 ml CEL-sol (0.32 mg/kg) every 2 d Rabbits were weighed every 4 d during CEL administration ($n = 5$). After 21 d, the rabbits were sacrificed to obtain the blood and major organs (hearts, livers, spleens, kidneys, brain). The level of alanine aminotransferase (ALT), aspartate aminotransferase (AST), lactate dehydrogenase (LDH), creatine kinase-MB (CKMB), creatinine (CREA), uric acid (UA), total bilirubin (BILT) in serum were analyzed by an auto biochemical analyzer (Hitachi, Japan). Red blood cell count (RBC), white blood count (WBC),

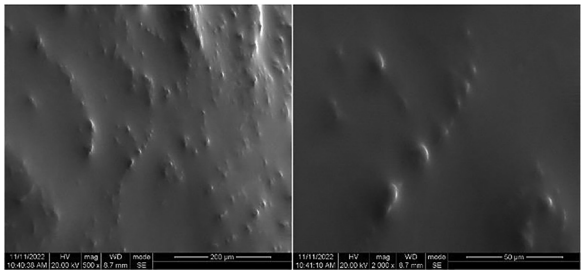

Fig. 2 – SEM (500 × and 2000 ×) of CEL-gel after phase transition *in vivo*.

and platelet count (PLT) of the whole blood were assayed on an auto hematology analyzer (Mindray BC-2800Vet, China). H&E staining of major organs was carried out to assess the toxicity of CEL.

2.10. *Statistical analysis*

All data were represented as mean ± standard deviation (SD). The *t*-test was used to assess comparisons between the two groups. One-way ANOVA was used to assess comparisons among multiple groups. A *P-value less than 0.05 was considered to be statistically different.

3. Results and discussion

3.1. *Preparation and characterization of CEL-gel*

The morphology of CEL-gel before and after gelation was shown in Fig. 1B-1C. Pre-CEL-gel was displayed in a clear and transparent solution with good fluidity and low viscosity (< 300 cP), suggesting that all excipients were well dissolved into this homogeneous mixture and conducive to injection [40,41]. After gelation, it transited to a gel state with less fluidity and a significantly increased viscosity (> 1000 cP) (Fig. 1D). As shown in Fig. 1E, the viscosity of pre-CEL-gel increased with the rise of phospholipid concentration. When the S100 content exceeds 70%, the viscosity is higher than 300 cP, making injection difficult. However, according to our previous research, the high concentration of phospholipid was the premise to maintain long-term sustained release [26]. Thus, a 70% phospholipid concentration in the CEL-gel was selected in our study.

Fig. 2 shows the SEM images of the *in vivo* injected CEL-gel. With the exchange of ethanol-synovial fluid, the external precipitated phospholipids form a film barrier that blocks the release of the drug. During the following time, the CEL was slowly released as phospholipids were progressively degraded in the body.

3.2. In vitro *release study*

Due to the extremely slow release of CEL from the CEL-gel in PBS release medium. 3% DMSO, 30% ethanol, or 50% ethanol was added in PBS (v/v) to stimulate the erosion of the CEL-gel and dissolution of the CEL. Fig. 3A showed the cumulative release profile of CEL. For the CEL-sol group, the release of CEL was fast in two ethanol-contained mediums with 100% CEL release in 6 h and in 2 d respectively, and in 3% DMSO-PBS medium with 100% release in 6 d In contrast, the release of CEL-gel was significantly slower. Less than 10% CEL was released from CEL-gel in 22 d in 3% DMSO-PBS. Nearly 50% CEL was released in 22 d in 30% ethanol-PBS medium, and there was 90% CEL release in 22 d when the ethanol content in PBS reached 50%. Since S100 was well soluble in ethanol, adding ethanol to the release medium accelerated the corrosion and diffusion of the gel system. These results suggested that CEL-gel effectively blocks CEL release due to the insoluble nature of S100 and MCT in the aqueous environment.

3.3. *Pharmacokinetic study*

The blood concentration-time profiles of CEL-gel and CEL-sol after IA injection in healthy rabbits were shown in Fig. 3B. Table 2 illustrates the corresponding pharmacokinetic parameters. CEL-sol showed a remarkable initial burst release of CEL in 2.5 h, and the high maximum blood concentration (C_{max}) of CEL was up to 282.67 μg/l. In contrast, CEL-gel kept a slower and steadier release of CEL as we expected, with the C_{max} just 18.44 μg/l. As we all know, initial burst release is almost a ubiquitous phenomenon for sustained controlled-release delivery systems, a high burst release would bring a risk of side effects or even toxic effects [42–44]. So, the IA injection of CEL-gel might improve the systemic safety of CEL. CEL-sol was rapidly eliminated *in vivo* (about 1 d) with a short half-time ($T_{1/2}$, 8.73 h), while CEL-gel sustainably released CEL for 25 d with a prolonged $T_{1/2}$ of 227.08 h. CEL-gel displayed approximately 36-fold and 4-fold increases of $MRT_{0-\infty}$ (Mean residence time) and $AUC_{0-\infty}$ (Area under the curve) compared to CEL-sol, indicating a long-time sustained delivery and improvement in bioavailability of CEL. In addition, we speculated that CEL would stay longer and be more concentrated in the local joint than in the blood because of local ethanol-synovial fluid exchange.

3.4. *Storage stability investigation*

The storage stability of pre-CEL-gel at 4 °C was evaluated by CEL content, drug-dispersion uniformity and viscosity. As shown in Fig. 4A, there was no change in the appearance of pre-CEL-gel after storage 28 d Data from quantitative HPLC analysis revealed that CEL content in the gel at different timepoint was no significant difference (Fig. 4B). The CEL concentrations at the upper or lower parts of the gel were equal, and the ratio remained steady in 28 d (Fig. 4C). In addition, viscosity was also unchanged before and after storage (Fig. 4D). These results indicated that the CEL was stable in gel and could be stored for at least a month, and the long-term stability might enable CEL-gel for clinical application.

S100 is a soybean phospholipid with a purity close to 100% of phosphatidylcholine, and its storage stability is mainly related to oxidation. As a result, after adding pre-CEL-gel to the bottle, the liquid surface was filled with argon to prevent S100 oxidation.

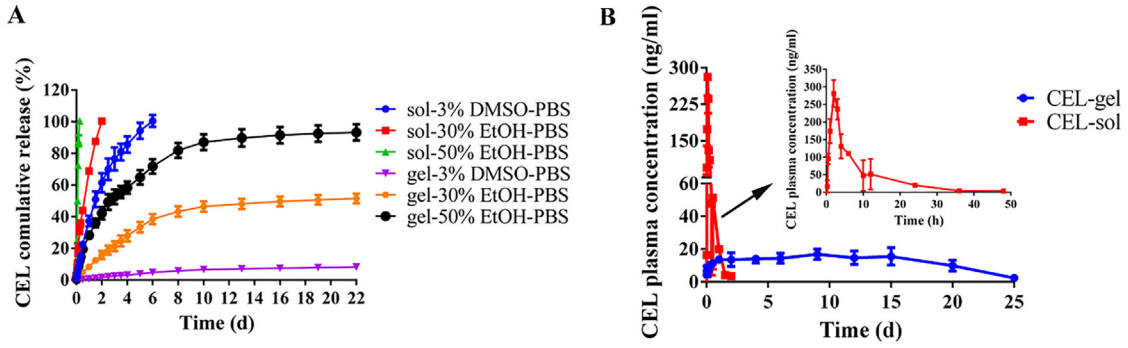

Fig. 3 – (A) *In vitro* release profile of CEL from CEL-gel and CEL-sol in various release mediums (n = 3). (B) *In vivo* pharmacokinetic profiles after a single IA injection of CEL-gel and CEL-sol in two joints (n = 5).

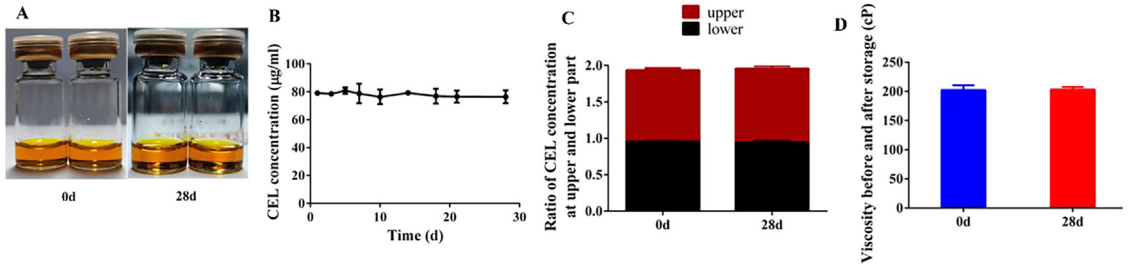

Fig. 4 – *In vitro* stability of pre-CEL-gel storage at 4 °C (n = 3). (A) Appearance before (0 d) and after (28 d) storage. (B) CEL content in pre-CEL-gel at different storage time points. (C) The ratio of CEL content at the upper and lower part of pre-CEL-gel after 28 d of storage. (D) Viscosity before (0 d) and after (28 d) storage. Values are expressed as mean ± SD.

Table 2
***In vivo* pharmacokinetic parameters after a single IA injection of CEL-gel and CEL-sol. Data are presented as mean ± SD (n = 5).**

Group	AUC (0-∞) (μg/l·h)	MRT $_{(0-\infty)}$ (h)	T $_{1/2}$ (h)	T_{max} (h)	C_{max} (μg/l)
CEL - sol	2054.83 ± 357.96	9.71 ± 0.52	8.73 ± 3.95	2.5 ± 0.71	282.67 ± 36.11
CEL - gel	8033.84 ± 750.16	352.4 ± 102.09	227.08 ± 127.98	232. 00 ± 163.36	18.78 ± 0.97

3.5. In vivo *therapeutic efficacy evaluation*

The AIA rabbit model shared some characteristics such as inflammation, cartilage destruction, and loss of joint function with human RA [45,46]. And the AIA rabbit offers an ideal animal model for studying IA drug administration since it has enough joint cavity space. However, slight arthritis induced by a single OVA solution without CFA IA injection would heal itself quickly [47], making it unsuitable for long-term formulation studies. In our experiment, we combined CFA with OVA to inject it into the rabbit joint cavity, building the severe AIA model that lasted for several months. The mechanism of the AIA model induced by OVA and CFA is that antibodies are generated by repeated SC injection. When the antigen was injected again into the joint cavity, the antigen was combined with antibodies and deposited on the cartilage and synovial to stimulate the complement system and cellular immunity of the body [48].

Articular skin temperature and joint swelling are key clinical signs in patients with RA, which are induced by local inflammatory responses and synovial hyperplasia [49]. In our study, we recorded joint diameter and joint skin temperature after CEL administration. As shown in Fig. 5B and 5C, the swelling of the joint treated with CEL-gel was significantly restrained compared to the saline group, while the CEL-sol group showed a poor improvement effect. However, those swelling improvement was limited, and joint diameter was observed to be gradually increased even under CEL administration, suggesting that IA delivery of CEL could alleviate but not eliminate serious inflammation and synovial hyperplasia caused by OVA/CFA emulsions. In addition, the CEL-gel and CEL-sol were discovered to tend toward lower knee surface temperatures compared with the saline group.

3.5.1. *CEL-gel improves inflammatory microenvironment*

The signaling factor NF-κB plays a key pathogenic role in the development of RA [50,51]. A stimulus such as immune complexes or cytokines activates NF-κB, thus promoting the transcription of multiple inflammatory cytokines, including TNF-α, IL-6, and IL-1β genes. This ultimately leads to progressive damage of the joint tissues caused by MMP-3 and

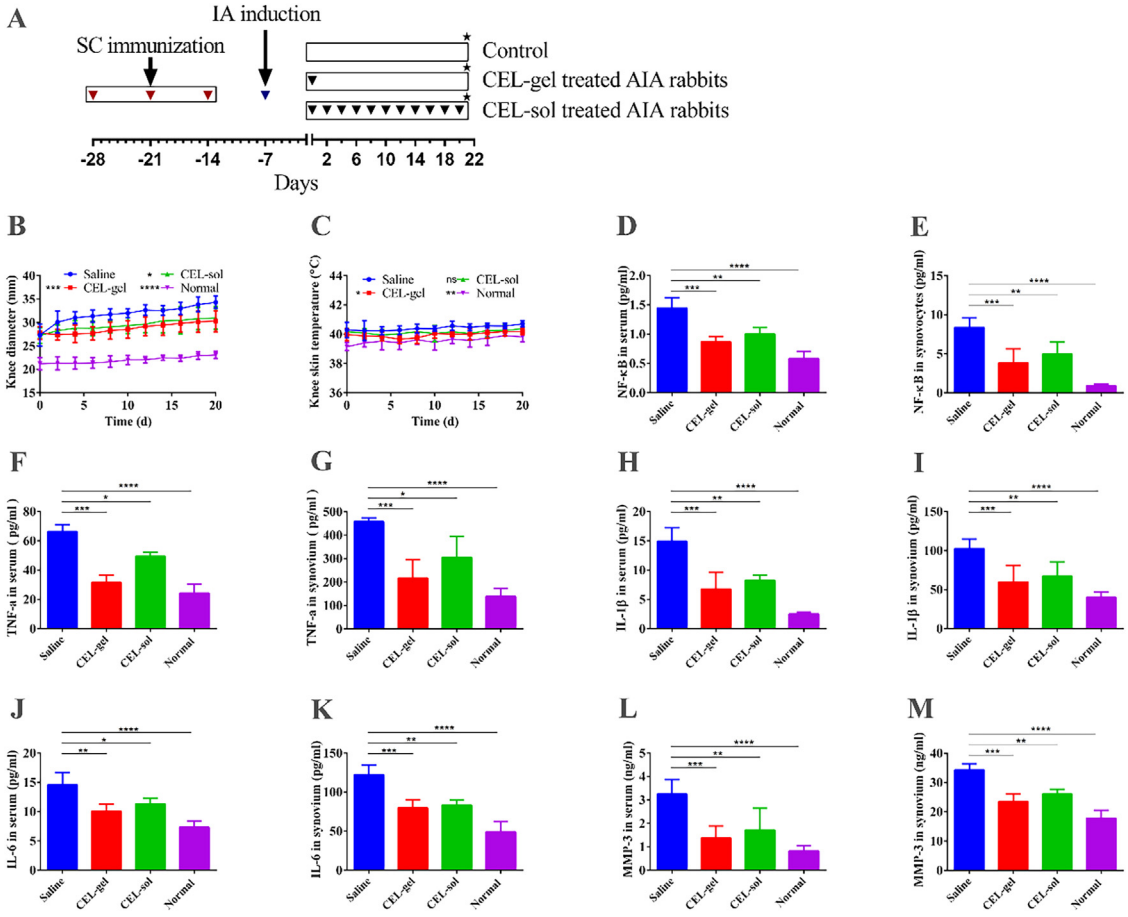

Fig. 5 – *In vivo* pharmacodynamic assessment. (A) Flow diagram of the experimental process of arthritis induction and IA treatment in rabbits. The red inverted triangle denotes SC immunization. The blue inverted triangle denotes IA arthritis induction. The black inverted triangle denotes IA injection of CEL-gel or CEL-sol. The black star denotes the treatment endpoint that rabbits were sacrificed. The trend of joint diameter (B), and knee skin temperature (C) in the process of different treatments ($n = 12$). (D-E) NF-κB express levels in serum and joint from the different treatment groups. (F-G) Quantification of TNF-α level in serum and joint from the different treatment groups. (H-I) Quantification of IL-1β level in serum and joints. (J-K) Quantification of IL-6 level in serum and joints. (L-M) MMP-3 secreted level in serum and joints ($n = 6$). Values are mean ± SD. *P < 0.05, **P < 0.01, ***P < 0.001.

other effect molecules. The secretion of NF-κB and levels of TNF-α, IL-6, IL-1β, and MMP-3 were measured to evaluate disease progression and therapy efficiency. In our study, serum was tested for systemic assessment, and the synovial homogenate was tested for local assessment. As shown in Fig. 5D-5E, compared to the saline group, the expression of NF-κB was greatly restrained in blood and local joints after the injection of CEL-gel. This restraint also occurred in the CEL-sol group but with less effectiveness. Analogously, the group treated with CEL-gel had lower concentrations of TNF-α, IL-6, and IL-1β compared to CEL-sol, while the group given saline produced the highest amounts of these cytokines (Fig. 5F-5K). These results further confirmed that CEL-gel could inhibit the inflammatory process. In addition, the lower concentration of MMP-3 (Fig. 5L-5M) in both serum and local joints further explained the protective effect of CEL-gel on cartilage degradation.

3.5.2. *CEL-gel significantly improves histopathology of knee joints* in vivo

To demonstrate that CEL-gel is capable of controlling inflammation and reducing cartilage degradation, histological analysis of rabbit knee joints was performed at the end of the study (Fig. 6A-6B). H&E-stained in the saline group showed severe cartilage destruction and trabecular collapse, with significant fibrous and vascular hyperplasia in addition to the infiltration of inflammatory cells. CEL-sol had only a modest impact on easing these symptoms and was accompanied by synovial hyperplasia protruding into the articular cavity and fibrous layer fracture, which might attribute to the frequent injection of free drug into the articular cavity. Surprisingly, CEL-gel significantly improved these symptoms compared with the saline group. Toluidine blue staining also showed that the cartilage in the saline group was seriously damaged, with a significantly reduced cartilage area. The cartilage in the

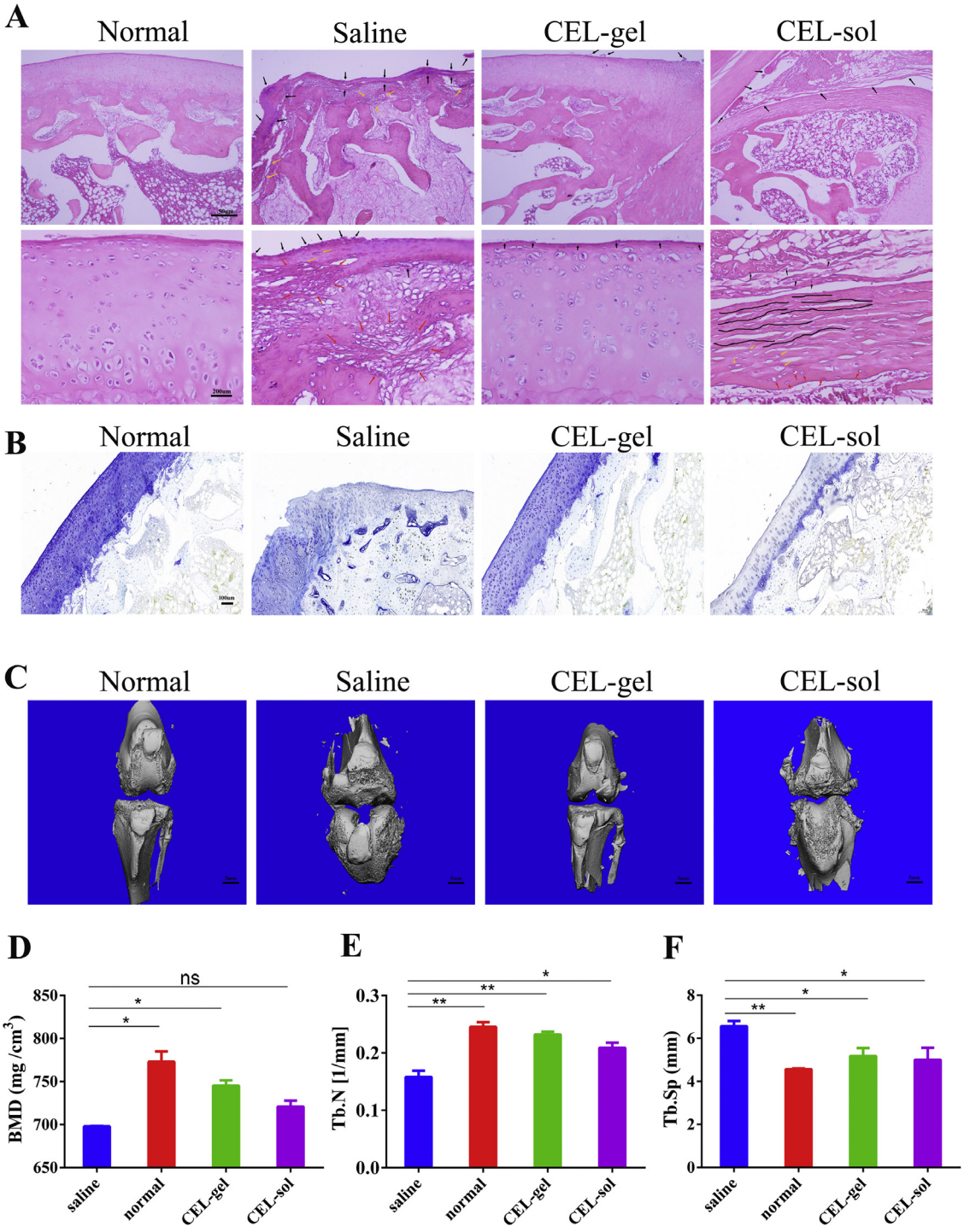

Fig. 6 – *In vivo* pharmacodynamic assessment. The knee joint histopathology was evaluated using (A) H&E -stained and (B) Toluidine blue stained ($n = 6$). (C) Micro-CT pictures of the keen joints after treatments. (D) Quantitative micro-CT analysis of BMD, (E) trabecular number (Tb. N), and (F) trabecular separation (Tb. Sp) ($n = 6$). Values are mean ± SD. *$P < 0.05$, **$P < 0.01$, ***$P < 0.001$.

CEL-gel group, however, stayed intact and was close to the normal group. Whereas the cartilage in CEL-sol was shown to be intermediate to that of the saline and CEL-gel groups. These results demonstrated that CEL-gel effectively reduced cartilage destruction and bone tissue damage.

Hyaluronic acid (HA) as the viscosupplementation in weight-bearing joints has been widely accepted in clinical practice [20]. Similar to the HA, phospholipids with elastic and viscous properties might also maintain lubrication in the joint. It has been reported that the addition of phospholipids

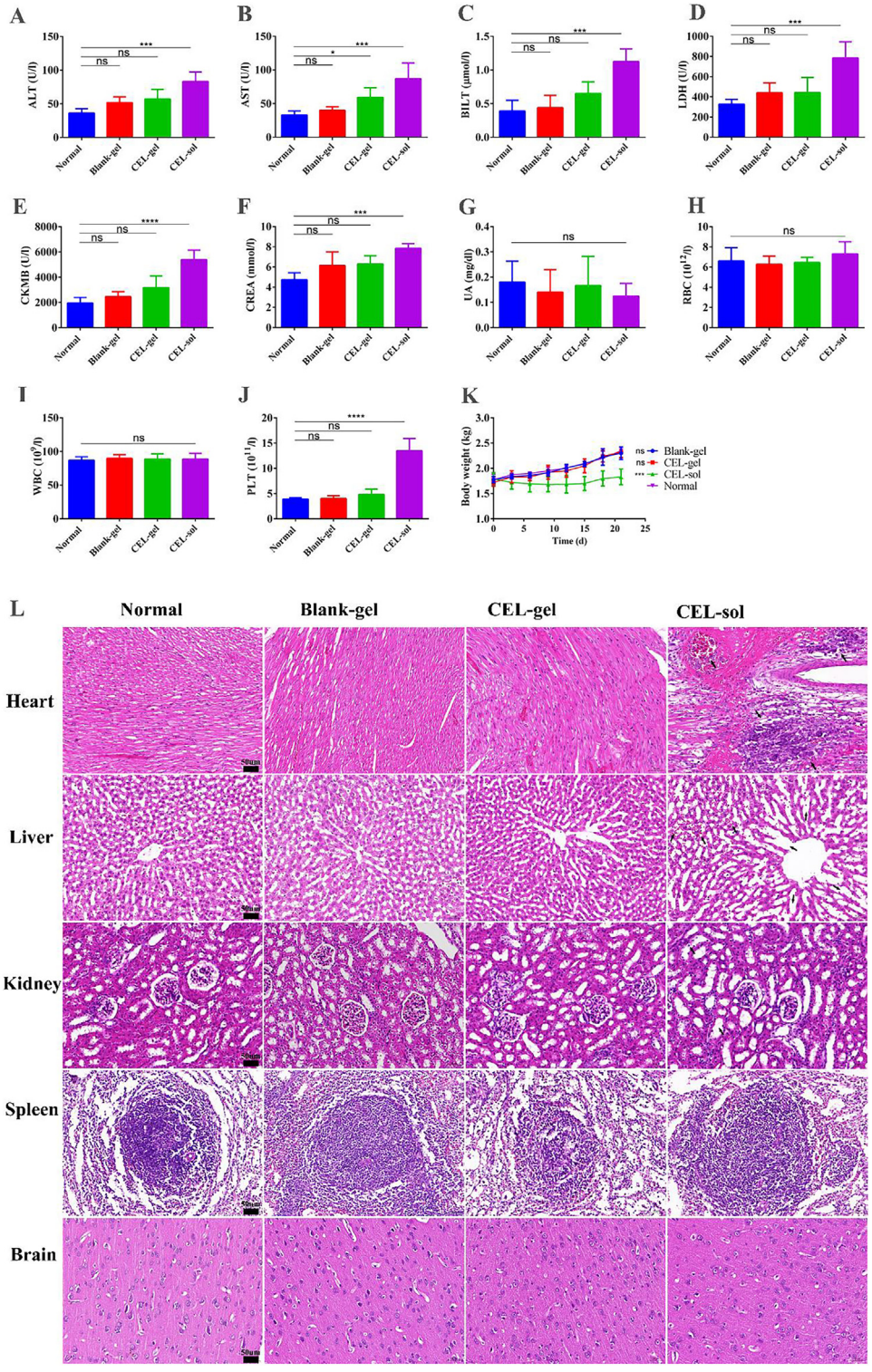

Fig. 7 – Safety evaluation of CEL-gel in rabbits. (A-G) Blood biochemical indexes from different groups. (H-J) Blood cell analysis from different groups. (K) Body weight of rabbits over time ($n = 5$). Values are mean ± SD. (L) H&E-stained pictures of the heart, liver, spleen, kidney and brain from different groups ($n = 5$). *P < 0.05, **P < 0.01, ***P < 0.001.

in HA solution indeed significantly improved the boundary lubricating ability of the articular surfaces [52–56]. It appears that the phospholipids could form protective films on the articular surfaces as a bio-membrane, as we all know, phospholipids are structural components of natural cell membranes [54]. Consequently, we hypothesized that the oily viscoelastic fluid CEL-gel, apart from the anti-inflammatory effect of CEL, S100 and MCT could also be a boundary lubricant after IA injection, thus further protecting articular cartilage from degenerative change.

3.5.3. *CEL-gel terminates the bone erosion*

The AIA rabbit model that we constructed shared some of the same characteristics as RA in the clinic, including the terminal symptom of bone erosion. On Day 21 after the intervention, a micro-CT scan of the knee joint was performed (Fig. 6C). The saline group exhibited coarse bone surfaces and osseous erosion, with a reduction in bone mineral density (BMD) (Fig. 6D) and destruction in the trabecular of the bone (Fig. 6E-6F) contrasted to the normal group. CEL-sol reduced trabecular damage moderately, with a slight increase in trabecular number (Tb. N) and a decrease in trabecular separation (Tb. Sp). Surprisingly, the CEL-gel group had smoother bone surfaces and higher BMD than the CEL-sol group. The trabecular bone parameters also affirmed that CEL-gel was efficient in increasing the Tb. N while decreasing the Tb. Sp. All these results indicated that CEL-gel could halt the advancement of bone damage.

3.6. *CEL-gel reduces systemic toxicity of CEL in rabbits*

A comprehensive safety evaluation was necessary to verify that CEL-gel reduces the toxicity of CEL in the hepatic, nephritic and cardiovascular systems. In our study, biochemical indicators (Fig. 7A-7G) demonstrated that gel-vehicle could mitigate cardiotoxicity (LDH, CKMB), hepatotoxicity (ALT, AST, BILT), and nephrotoxicity (UREA) of CEL. Whole blood tests for Blank-gel and CEL-gel groups also showed no significant alteration in WBC, RBC, and PLT levels, while the CEL-sol group with significantly increased PLT levels (Fig. 7H-7J).

Histological analysis (Fig. 7L) for major organs further proved the safety of CEL-gel. CEL-sol exhibited serious cardiotoxicity, including myocardial fiber necrosis, myocytes nucleus shrinks, and interstitial hyperemia. As well as causing severe liver congestion and hepatic sinus dilatation. Additionally, renal tubules dilation and epithelial cells exfoliation were also observed in the CEL-sol group. While animals exposed to blank-gel or CEL-gel showed no visible lesions in the main organs, implying low systemic toxicity for both blank-gel and CEL-gel. Repeat IA injection of free CEL also affected rabbits weight gain, while this phenomenon did not occur in CEL-gel treated group (Fig. 7K). These results suggested that CEL-gel was a secure drug delivery system that could assist in lowering the systematic toxicity of the drug.

4. Conclusion

For the treatment of large joint arthritis, we created a unique IA injectable phospholipids-based gel for local sustained delivery of CEL. It was prepared by a simple magnetic agitation method and has safe and biodegradable formulation components. The gel delivery system was an injectable solution with low viscosity *in vitro*, after being injected *in vivo*, it spontaneously performed sol-gel transition to form a drug depot in the joint cavity, achieving the gradual release of CEL as the gel skeleton degraded in the body. A single IA injection could provide 25 d of sustained CEL release, improving CEL bioavailability while decreasing toxicity. The pharmacodynamic study also proved the superior anti-inflammation efficiency of CEL-gel in the AIA rabbit model. With these advantages, we believe CEL-gel has the potential to be used in clinical arthritis treatment.

Conflicts of interest

The authors declared that they have no conflict of interest in this study.

Acknowledgments

This work was financially supported by the National Natural Science Foundation of China (Nos. 82173758, China) and Sichuan major science and technology project on biotechnology and medicine (2018SZDZX0018, China). We appreciate Dr. Li Chen (Analytical and Testing Center Sichuan University) for providing micro-CT scanning and analysis.

References

[1] Yeo L, Adlard N, Juarez M, Smallie T, Snow M, Buckley CD, et al. Expression of chemokines CXCL4 and CXCL7 by synovial macrophages defines an early stage of rheumatoid arthritis. Ann Rheum Dis 2016;75:763–71.
[2] Arend WP. Physiology of cytokine pathways in rheumatoid arthritis. Arthritis Care Res 2001;45:101–6.
[3] Choy EHS, Panayi GS. Cytokine pathways and joint inflammation in rheumatoid arthritis. N Engl J Med 2001;344:907–16.
[4] Smolen JS, Aletaha D, McInnes IB. Rheumatoid arthritis. Lancet 2016;388:2023–38.
[5] Ghosh S, Karin M. Missing pieces in the NF-κB puzzle. Cell 2002;109:S81–96.
[6] Allison AC, Cacabelos R, Lombardi VRM, Alvarez XA, Vigo C. Celastrol, a potent antioxidant and anti-inflammatory drug, as a possible treatment for Alzheimer's disease. Prog Neuropsychopharmacol Biol Psychiatry 2001;25:1341–57.
[7] Wong K-F, Yuan Y, Luk JM. Tripterygium wilfordii bioactive compounds as anticancer and anti-inflammatory agents. Clin Exp Pharmacol Physiol 2012;39:311–20.
[8] Sethi G, Ahn KS, Pandey MK, Aggarwal BB. Celastrol, a novel triterpene, potentiates TNF-induced apoptosis and suppresses invasion of tumor cells by inhibiting NF-κB–regulated gene products and TAK1-mediated NF-κB activation. Blood 2007;109:2727–35.
[9] Deng CF, Zhang Q, He PH, Zhou B, He K, Sun X, et al. Targeted apoptosis of macrophages and osteoclasts in arthritic joints is effective against advanced inflammatory arthritis. Nat Commun 2021;12.

[10] Wong VKW, Qiu CL, Xu SW, Law BYK, Zeng W, Wang H, et al. Ca^{2+} signalling plays a role in celastrol-mediated suppression of synovial fibroblasts of rheumatoid arthritis patients and experimental arthritis in rats. Br J Pharmacol 2019;176:2922–44.
[11] Cascao R, Vidal B, Carvalho T, Lopes IP, Romao VC, Goncalves J, et al. Celastrol efficacy by oral administration in the adjuvant-induced arthritis Model. Front Med 2020;7:455.
[12] Astry B, Venkatesha SH, Laurence A, Christensen-Quick A, Garzino-demo A, Frieman MB, et al. Celastrol, a Chinese herbal compound, controls autoimmune inflammation by altering the balance of pathogenic and regulatory T cells in the target organ. Clin Immunol 2015;157:228–38.
[13] Cascão R, Vidal B, Raquel H, Neves-Costa A, Figueiredo N, Gupta V, et al. Effective treatment of rat adjuvant-induced arthritis by celastrol. Autoimmun Rev 2012;11:856–62.
[14] Wang S, Liu K, Wang X, He Q, Chen X. Toxic effects of celastrol on embryonic development of zebrafish (Danio rerio). Drug Chem Toxicol 2011;34:61–5.
[15] Guo L, Luo S, Du Z, Zhou M, Li P, Fu Y, et al. Targeted delivery of celastrol to mesangial cells is effective against mesangioproliferative glomerulonephritis. Nat Commun 2017;8:878.
[16] Zhang J, Li CY, Xu MJ, Wu T, Chu JH, Liu SJ, et al. Oral bioavailability and gender-related pharmacokinetics of celastrol following administration of pure celastrol and its related tablets in rats. J Ethnopharmacol 2012;144:195–200.
[17] Zhang X, Zhang T, Zhou X, Liu H, Sun H, Ma Z, et al. Enhancement of oral bioavailability of tripterine through lipid nanospheres: preparation, characterization, and absorption evaluation. J Pharm Sci 2014;103:1711–19.
[18] Gerwin N, Hops C, Lucke A. Intraarticular drug delivery in osteoarthritis. Adv Drug Deliver Rev 2006;58:226–42.
[19] Okuyama S, Aihara H. The mode of action of analgesic drugs in adjuvant arthritic rats as an experimental model of chronic inflammatory pain: possible central analgesic action of acidic nonsteroidal antiinflammatory drugs. Jpn J Pharmacol 1984;35:95–103.
[20] Antonio G, Leonardo C. The role of intra-articular hyaluronan (Sinovial®) in the treatment of osteoarthritis. Rheumatol Int 2011;31:427–44.
[21] Kolasinski SL, Neogi T, Hochberg MC, Oatis C, Guyatt G, Block J, et al. 2019 American college of rheumatology/arthritis foundation guideline for the management of osteoarthritis of the hand, hip, and knee. Arthritis Care Res 2020;72:149–62.
[22] Bucci J, Chen X, LaValley M, Nevitt M, Torner J, Lewis CE, et al. Progression of knee 0steoarthritis with use of intraarticular glucocorticoids *versus* hyaluronic acid. Arthritis Rheumatol 2022;74:223–6.
[23] Wenzel JGW, Balaji KSS, Koushik K, Navarre C, Duran SH, Rahe CH, et al. Pluronic (R) F127 gel formulations of Deslorelin and GnRH reduce drug degradation and sustain drug release and effect in cattle. J Controlled Release 2002;85:51–9.
[24] Song YH, Gao JP, Xu XY, Zhao HL, Xue RN, Zhou JK, et al. Fabrication of thermal sensitive folic acid based supramolecular hybrid gels for injectable drug release gels. Mater Sci Eng C 2017;75:706–13.
[25] Kim S, Lee HJ, Jeong B. Hyaluronic acid-g-PPG and PEG-PPG-PEG hybrid thermogel for prolonged gel stability and sustained drug release. Carbohydr Polym 2022;291:119559.
[26] Zhang T, Peng Q, San FY, Luo JW, Wang MX, Wu WQ, et al. A high-efficiency, low-toxicity, phospholipids-based phase separation gel for long-term delivery of peptides. Biomaterials 2015;45:1–9.
[27] Wu W, Chen H, Shan F, Zhou J, Sun X, Zhang L, et al. A novel doxorubicin-loaded *in situ* forming gel based high concentration of phospholipid for intratumoral drug delivery. Mol Pharm 2014;11:3378–85.
[28] Larsen SW, ØStergaard J, Friberg-Johansen H, Jessen MNB, Larsen C. *In vitro* assessment of drug release rates from oil depot formulations intended for intra-articular administration. Eur J Pharm Sci 2006;29:348–54.
[29] Shan-Bin G, Yue T, Ling-Yan J. Long-term sustained-released *in situ* gels of a water-insoluble drug amphotericin B for mycotic arthritis intra-articular administration: preparation, *in vitro* and *in vivo* evaluation. Drug Dev Ind Pharm 2015;41:533–50.
[30] Wang M, Shan F, Zou Y, Sun X, Zhang ZR, Fu Y, et al. Pharmacokinetic and pharmacodynamic study of a phospholipid-based phase separation gel for once a month administration of octreotide. J Control Release 2016;230:45–56.
[31] Gong T, Tan T, Zhang P, Li H, Deng C, Huang Y, et al. Palmitic acid-modified bovine serum albumin nanoparticles target scavenger receptor-a on activated macrophages to treat rheumatoid arthritis. Biomaterials 2020;258:120296.
[32] Hu X, Jia M, Fu Y, Zhang P, Zhang Z, Lin Q. Novel low-toxic derivative of celastrol maintains protective effect against acute renal injury. ACS Omega 2018;3:2652–60.
[33] Wei G, Song X, Fu Y, Gong T, Zhang Q. Sustained-release mitochondrial protonophore reverses nonalcoholic fatty liver disease in rats. Int J Pharm 2017;530:230–8.
[34] Kaklamanis PM. Experimental animal models resembling rheumatoid arthritis. Clin Rheumatol 1992;11:41–7.
[35] Prieto-Potín I, Roman-Blas J, Martínez-Calatrava M, Gómez R, Largo R, Herrero-Beaumont G. Hypercholesterolemia boosts joint destruction in chronic arthritis. An experimental model aggravated by foam macrophage infiltration. Arthritis Res Ther 2013;15:R81.
[36] Romero FI, Martínez-Calatrava MJ, Sánchez-Pernaute O, Gualillo O, Largo R, Herrero-Beaumont G. Pharmacological modulation by celecoxib of cachexia associated with experimental arthritis and atherosclerosis in rabbits. Br J Pharmacol 2010;161:1012–22.
[37] Dekkers JS, Schoones JW, Huizinga TW, Toes RE, van der Helm-van Mil AH. Possibilities for preventive treatment in rheumatoid arthritis? Lessons from experimental animal models of arthritis: a systematic literature review and meta-analysis. Ann Rheum Dis 2017;76:458–67.
[38] Bagdonas S, Kirdaite G, Streckyte G, Graziene V, Leonaviciene L, Bradunaite R, et al. Spectroscopic study of ALA-induced endogenous porphyrins in arthritic knee tissues: targeting rheumatoid arthritis PDT. Photochem Photobiol Sci 2005;4:497–502.
[39] Okura T, Marutsuka K, Hamada H, Sekimoto T, Fukushima T, Asada Y, et al. Therapeutic efficacy of intra-articular adrenomedullin injection in antigen-induced arthritis in rabbits. Arthritis Res Ther 2008;10:R133.
[40] Long DH, Gong T, Zhang ZR, Ding R, Fu Y. Preparation and evaluation of a phospholipid-based injectable gel for the long term delivery of leuprolide acetaterrh. Acta Pharm Sin B 2016;6:329–35.
[41] Xuan JJ, Balakrishnan P, Oh DH, Yeo WH, Park SM, Yong CS, et al. Rheological characterization and *in vivo* evaluation of thermosensitive poloxamer-based hydrogel for intramuscular injection of piroxicam. Int J Pharm 2010;395:317–23.
[42] Ahmed AR, Dashevsky A, Bodmeier R. Drug release from and sterilization of *in situ* cubic phase forming monoglyceride drug delivery systems. Eur J Pharm Biopharm 2010;75:375–380.
[43] Kranz H, Bodmeier R. A novel *in situ* forming drug delivery system for controlled parenteral drug delivery - ScienceDirect. Int J Pharm 2007;332:107–14.
[44] Perpetuo IP, Caetano-Lopes J, Rodrigues AM, Campanilho-Marques R, Ponte C, Canhao H, et al. Methotrexate and low-dose prednisolone downregulate osteoclast function by

decreasing receptor activator of nuclear factor-kappabeta expression in monocytes from patients with early rheumatoid arthritis. RMD Open 2017;3:000365.
[45] Choudhary N, Bhatt LK, Prabhavalkar KS. Experimental animal models for rheumatoid arthritis. Immunopharmacol Immunotoxicol 2018;40:193–200.
[46] Hegen M, Keith JC, Collins M, Nickerson-Nutter CL. Utility of animal models for identification of potential therapeutics for rheumatoid arthritis. Ann Rheum Dis 2008;67:1505–1515.
[47] Henderson B, Higgs GA. Synthesis of arachidonate oxidation products by synovial joint tissues during the development of chronic erosive arthritis. Arthritis Rheum 1987;30:1149–56.
[48] Nandakumar KS. Pathogenic antibody recognition of cartilage. Cell Tissue Res 2010;339:213–20.
[49] Aletaha D, Neogi T, Silman AJ, Funovits J, Felson DT, Bingham CO, et al. 2010 Rheumatoid arthritis classification criteria: an American college of rheumatology/European league against rheumatism collaborative initiative. Ann Rheum Dis 2010;62:2569–81.
[50] Wang Q, Jiang H, Li Y, Chen W, Li H, Peng K, et al. Targeting NF-kB signaling with polymeric hybrid micelles that co-deliver siRNA and dexamethasone for arthritis therapy. Biomaterials 2017;122:10–22.
[51] Kawane K, Ohtani M, Miwa K, Kizawa T, Kanbara Y, Yoshioka Y, et al. Chronic polyarthritis caused by mammalian DNA that escapes from degradation in macrophages. Nature 2006;443:998–1002.
[52] Kawano T, Miura H, Mawatari T, Moro-Oka T, Nakanishi Y, Higaki H, et al. Mechanical effects of the intraarticular administration of high molecular weight hyaluronic acid plus phospholipid on synovial joint lubrication and prevention of articular cartilage degeneration in experimental osteoarthritis. Arthritis Rheum 2014;48:1923–9.
[53] Schwarz IM, Hills BA. Surface-active phospholipid as the lubricating component of lubricin. Rheumatology 1998;37:21–26.
[54] Higaki H, Murakami T, Nakanishi Y, Miura H, Mawatari T, Iwamoto Y. The lubricating ability of biomembrane models with dipalmitoyl phosphatidylcholine and gamma-globulin. Proc Inst Mech Eng Part H J Mech Eng Med 1998;212:337–46.
[55] Pasquali-Ronchetti I, Quaglino D, Mori G, Bacchelli B, Ghosh P. Hyaluronan–phospholipid interactions. J Struct Biol 1997;120:1–10.
[56] Cao Y, Ma Y, Tao Y, Lin W, Wang P. Intra-articular drug delivery for osteoarthritis treatment. Pharmaceutics 2021;13:2166.